CHAPTER II
LITERATURE REVIEW

2.1 Introduction

Since the early 2000s, considerable research has focused on incorporating recycled materials as substitutes in concrete production. This practice has become increasingly prominent in infrastructure development due to engineering, economic, and environmental advantages (Dosho, 2007; FHWA, 2004). Although many Asian countries possess abundant natural resources, the use of industrial by-products has steadily grown as the need to conserve raw materials, reduce waste disposal costs, and lower the carbon footprint of construction activities becomes more urgent. The extraction, crushing, transportation, and storage of natural aggregates demand substantial energy and contribute significantly to environmental degradation. Consequently, shifting toward the utilization of recycled and by-product materials presents an effective strategy for reducing reliance on virgin aggregates and promoting sustainable construction practices.

The integration of recycled materials into concrete production offers two principal benefits: it decreases the consumption of natural aggregates while alleviating waste management challenges, and it can also contribute to lowering construction costs. To support the widespread adoption of recycled alternatives, extensive studies have investigated the feasibility of using Recycled Concrete Aggregate (RCA) obtained from demolished structures as a substitute for natural aggregates, particularly for pavement applications.

2.2 Ordinary Portland Cement (OPC)

Ordinary Portland Cement (OPC) is a hydraulic cement composed mainly of calcium silicates, which harden through a chemical reaction with water to form a solid binder known as paste. When this paste is mixed with aggregates such as sand, gravel, or crushed stone, it binds the particles together to produce concrete—one of the most

widely used construction materials. Although the terms cement and concrete are often mistakenly used interchangeably, cement is only one component of concrete. Cement is a finely ground powder, whereas concrete is the resulting stone-like solid. Typically, cement accounts for approximately 7% to 15% of the total weight of concrete.

Portland cement, typically recognized as a fine gray powder, is composed of several hydraulic cement minerals, including tricalcium silicate, dicalcium silicate, tricalcium aluminate, and tetracalcium aluminoferrite. These constituents are identified by specific chemical formulas and abbreviated notations, as summarized in **Table 2.1.**

Table 2.1 the main composition of Portland cement.

Composition name	Chemical composition	initials
Tricalcium Silicate	$3CaO \cdot SiO_2$	C_3S
Dicalcium Silicate	$2CaO \cdot SiO_2$	C_2S
Tricalcium Aluminate	$3CaO \cdot Al_2O_3$	C_3A
Tetracalcium Aluminoferrite	$4CaO \cdot Al_2O_3 \cdot Fe_2O_3$	C_4AF

The production of Portland cement begins with selecting and proportioning raw materials, which are then crushed, ground, and prepared for pyroprocessing. Its main chemical constituents include calcium, silicon, aluminum, iron, and oxygen, with minor components—such as magnesium, sulfur, sodium, and potassium—making up less than 5% by weight. SEM images of Ordinary Portland Cement (OPC) are shown in **Figure 2.1,** and its physical and chemical properties are summarized in **Tables 2.2**.

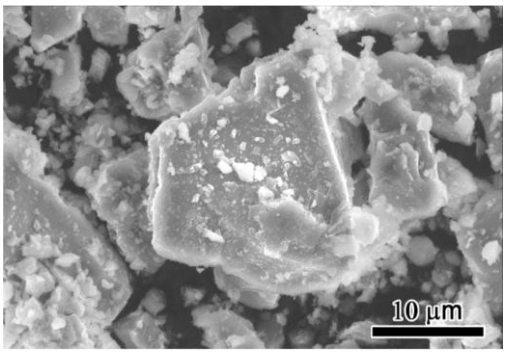

Figure 2.1 the SEM micrographs of OPC (Hongfang, 2015).

Tables 2.2 the physical and chemical properties of OPC (Hongfang, 2015).

Chemical Composition (%)	OPC
SiO_2	22.52
Al_2O_3	5.80
Fe_2O_3	3.52
SO_3	2.54
CaO	62.08
MgO	1.55
Na_2O	0.05
K_2O	0.56
LOI	0.94
Physical property	-
Specific gravity	3.12
Retained on sieve No. 325 (%)	4.70
BET surface area (m^2/g)	2.70
Median particle size, d50 (µm)	12.00

Cement plants operate using either the wet or dry process. The wet process mixes raw materials with water to form a slurry, whereas the dry process grinds them into a powder. Modern plants in the United States exclusively use the dry process due to its lower thermal energy demand (2.7–7.3 million Btu per ton). Thermal efficiency is further improved by incorporating cyclone preheaters and calciners.

Within the rotary kiln, raw materials undergo chemical reactions to form cement clinker, which is then cooled, blended with gypsum, and ground in mills to produce Portland cement. The final product is transported in bulk or packaged bags.

2.3 The Hydration Reactions

The four main cement minerals hydrate at different rates due to their distinct reactivities. Their behavior has been widely studied by hydrating each mineral in pure form under controlled conditions. Although, in actual cement hydration, all minerals dissolve into a common pore solution—meaning the resulting products cannot be linked to a single mineral—these individual studies still provide useful approximations for understanding overall hydration behavior.

2.3.1 Hydration of the calcium silicate minerals (C_3S and C_2S)

Tricalcium silicate (C_3S) is the primary and most influential mineral in Portland cement, contributing largely to its early-age strength. Its hydration reaction can be expressed as follows:

$$2(3CaO \cdot SiO_2) + 6H_2O \longrightarrow 3CaO \cdot 2SiO_2 \cdot 3H_2O + 3Ca(OH)_2$$

$$\text{Or : } 2C_3S+6H_2O \longrightarrow C_3S_2H_3+3Ca(OH)_2 \quad (2.1)$$

The dicalcium silicate phase (C_2S) reacts according to:

$$2(2CaO \cdot SiO_2) + 4H_2O \longrightarrow 3CaO \cdot 2SiO_2 \cdot 3H_2O + 3Ca(OH)_2$$

$$\text{Or : } 2C_2S+4H_2O \longrightarrow C_3S_2H_3+Ca(OH)_2 \quad (2.2)$$

The hydration products of C_2S are similar to those of C_3S but generate less $Ca(OH)_2$. Because C_2S is less soluble, it hydrates more slowly, contributing little to early strength but playing an important role in the long-term strength of hardened cement paste and concrete.

2.3.2 Hydration of the calcium aluminate/ferrite minerals (C_3A and C_4AF)

The hydration of aluminate and ferrite minerals is more complex than that of calcium silicates and is strongly affected by sulfate ions in the pore solution. C_3A is especially soluble—more so than C_3S—and when hydrated in pure water, it forms calcium aluminate hydrates through a characteristic reaction sequence:

$$3CaO \bullet Al_2O_3 + 6H_2O \longrightarrow 3CaO \bullet Al_2O_3 \bullet 6H_2O$$
$$\text{Or : } C_3A + 6H_2O \longrightarrow 3C_3AH_6 \quad (2.3)$$

The resulting compound, C_3AH_6, is commonly known as hydrogarnet. The initial hydration of C_3A is extremely fast, and without control it would release excessive heat and cause the paste to set within minutes—a phenomenon called flash set. To avoid this, gypsum ($CaSO_4 \cdot 2H_2O$) is added to cement. Because gypsum dissolves readily, it supplies calcium and sulfate ions to the pore solution, directing C_3A to follow an alternative, controlled hydration pathway. The reaction between C_3A and gypsum can be expressed as follows:

$$3CaO \bullet Al_2O_3 + CaSO_4 \bullet 2H_2O \longrightarrow 3CaO \bullet Al_2O_3 \bullet 3CaSO_4 + 31H_2O$$
$$\text{Or : } C_3A + \text{Gypsum} \longrightarrow \text{Ettringite} \quad (2.4)$$

Where $3CaO \bullet Al_2O_3 \bullet 3CaSO_4 + 31H_2O$ is the mineral Ettringite.

The ferrite phase (C_4AF) hydrates in a manner similar to C_3A but at a slower rate. A key distinction is that some aluminum in the hydration products is replaced by iron, with the degree of substitution depending on the C_4AF composition and the conditions in the paste. Early hydration involves reactions with gypsum ($CaSO_4 \cdot 2H_2O$) and calcium hydroxide ($Ca(OH)_2$), producing needle-like sulphoaluminate and sulphoferrite phases. These reactions can be represented as follows:

$$4CaO \bullet Al_2O_3 + Fe_2O_3 + CaSO_4 \bullet 2H_2O + Ca(OH)_2 \rightarrow 3CaO(Al_2O_3, Fe_2O_3) \bullet 3CaSO_4$$
$$\text{Or : } C_4AF + \text{Gypsum} + Ca(OH)_2 \rightarrow \text{Sulphoaluminate and Sulphoferrite} \quad (2.5)$$

2.3.3 Influence of the Compound Composition on Properties of Cement

C_3S and C_2S are the primary contributors to strength development in Portland cement. C_3S governs early strength gain during the first four weeks, whereas C_2S contributes mainly beyond this period. After about one year, their contributions to ultimate strength become comparable. C_3A increases early strength within the first

three days but may lead to later strength reductions, particularly in cements high in C_3A or in total (C_3A + C_4AF). The role of C_4AF in strength development remains uncertain and is generally considered minimal. The compressive strength development of these compounds over time is shown in **Figure 2.2**.

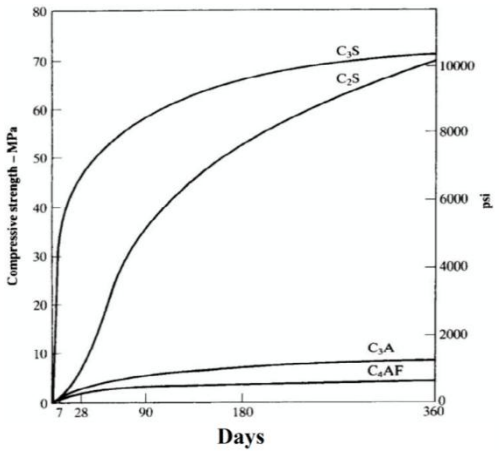

Figure 2.2 Contribution of Compressive strength of C_3S, C_2S, C_3A and C_4AF with time (Lerch, 2008)

2.3.4 Calcium-Silicate-Hydrate (C-S-H) gel

C–S–H gel is the dominant hydration product in cement paste, accounting for roughly 50% of its volume. Although not inherently strong, it forms a continuous binding phase that holds cement particles together (see Figure 2.3). Unlike other hydration products that appear as isolated crystals, C–S–H derives its binding capability from its nanoscale structure. Key characteristics of C–S–H include its internal pore system and its two primary morphologies, which are discussed in more detail in a later section.

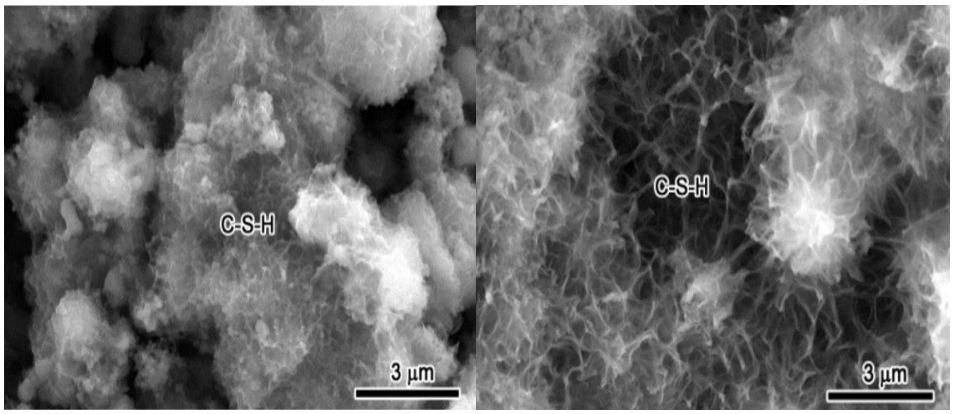

Figure 2.3 The SEM images of C-S-H structure (Li, 2015).

As C–S–H gel forms around cement grains, it creates a network of extremely fine gel pores that are much smaller than the original capillary pores. The water within these gel pores becomes physically trapped and does not participate in further hydration, resulting in variable water contents within the gel. Because C–S–H occupies more volume than the original C_3S and C_2S, its growth causes the layers to interconnect and form a continuous solid phase, leading to the setting and hardening of the paste. Since the overall paste volume changes little after mixing, this increase in solid volume reduces and disrupts the capillary pore network—particularly at low water-to-cement ratios. Consequently, the permeability of the cement paste decreases, improving its resistance to liquid water and ion penetration.

2.3.5 Calcium Hydroxide (CH)

Calcium hydroxide, or portlandite, is produced during the hydration of C_3S and C_2S and typically makes up about 15% of the volume of Portland cement paste. Its crystals vary in shape and size depending on the available space for growth. When formed in capillary pores, they often appear as irregular hexagonal plates several microns wide, which can be seen under an optical microscope. (refer to **Figure 2.4**).

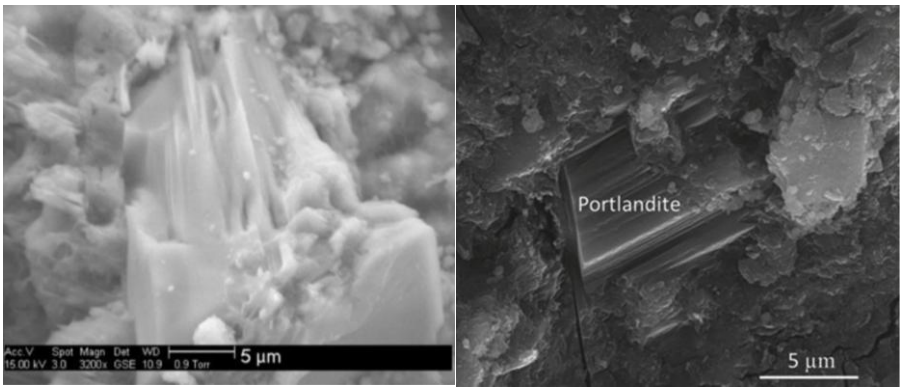

Figure 2.4 The SEM images of CH structure (Wang, 2008; Frias, 2015).

Besides forming larger plate-like crystals, calcium hydroxide (CH) can also appear as much smaller crystals that grow within and interact with low-density C–S–H. These fine CH crystals, often less than 1 µm, are restricted by the surrounding solid matrix. Studies also indicate the presence of nanometer-scale CH in cement paste, consistent with the nanoscale morphology of C–S–H formed alongside it. At this scale, distinguishing CH from C–S–H becomes difficult because C–S–H also contains many Ca–OH bonds.

2.3.6 Calcium trisulfoaluminate hydrate (Ettringite)

When cement first comes into contact with water, hydration begins quickly. Gypsum dissolves early, after which the remaining tricalcium aluminate (C_3A) reacts with the ettringite formed initially (**Figure 2.5a**) to produce calcium monosulfoaluminate ($3CaO{\cdot}Al_2O_3{\cdot}CaSO_4{\cdot}12H_2O$), as shown in Figure 2.5b. Monosulfoaluminate occupies less volume than ettringite and remains stable unless additional sulfate becomes available. If extra sulfate enters the system, it can react with monosulfoaluminate to reform ettringite, causing expansion—this is the basis of sulfate attack in hardened concrete exposed to external sulfate sources.

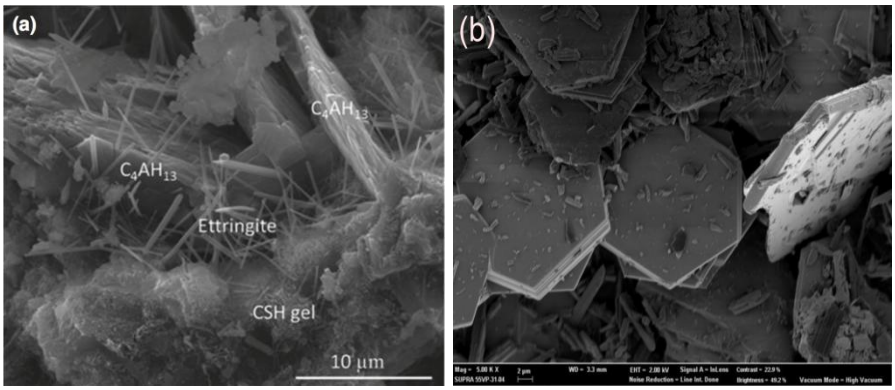

Figure 2.5 The SEM images of (a) Ettringite (Frias, 2015) (b) Monosulfate (Choi, 2012)

Locher et al. (1974) described the formation of hydration products and the development of cement paste structure after mixing. They identified three distinct stages that characterize the hydration process and the evolution of the paste structure, as illustrated in **Figure 2.6**.

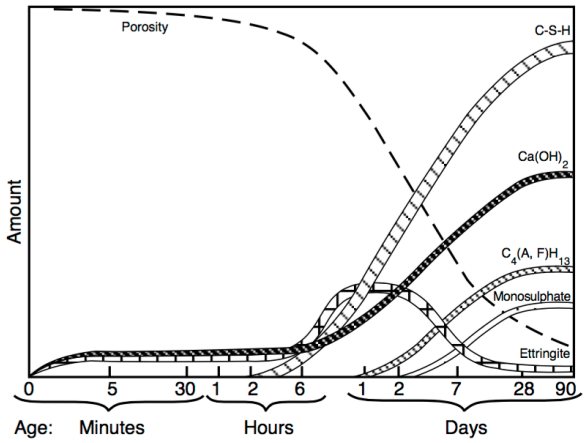

Figure 2.6 Formation of the of hydration products and the creation of cement paste structure (Locher, 1974)

2.4 General features

The hydration products in cement paste are not separate phases but are interwoven at micro- to nanoscale levels, except for high-density C–S–H that forms within the original cement grains. Thus, descriptions of cement paste microstructure focus on the distribution of solid phases and porosity rather than the structure of

individual hydrates. A useful and simplified representation divides the microstructure into three primary phases, as shown in **Figure 2.7**.

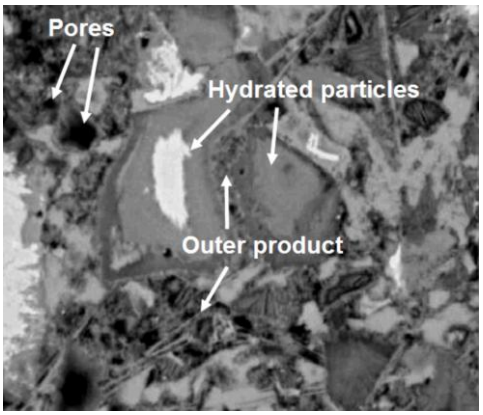

Figure 2.7 Backscattered SEM image of a mature cement paste showing the main microstructural features. (Image courtesy of Paul Stutzmann, Concrete Microscopy Library).

2.4.1 The interfacial transition zone (ITZ): In fresh concrete, the packing of cement particles near large solid inclusions, such as aggregates, is disrupted by the well-known "wall effect." This disturbance is intensified during mixing, as aggregates impose shear forces that cause water to separate from the cement particles. As a result, a thin region forms around each aggregate with fewer cement particles and more water. This area is known as the interfacial transition zone (ITZ), as shown in **Figure 2.8**.

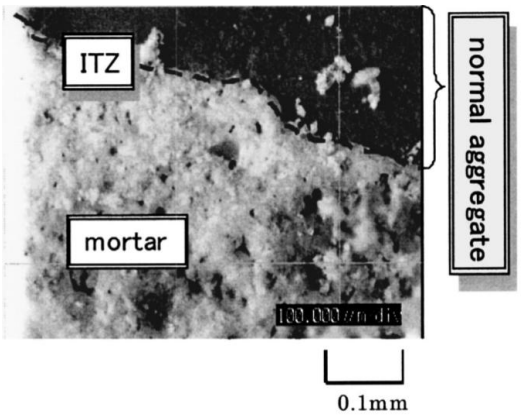

Figure 2.8 The ITZ between mortar and aggregate in concrete (Otsuki, 2003).

2.4.5 Effect of w/c Ratio

Kim et al. (2014) reported that adding more mixing water improves the workability of cement mortar but also increases porosity, leading to reduced durability and structural performance. Higher water content produces a coarser pore structure. As shown in Figure 2.13, increasing the w/c ratio from 0.45 to 0.60 raises porosity by up to 150% while lowering compressive strength to about 75.6%. Similar trends were noted by Albano et al. (2009), Ait-Aider et al. (2007), Ma et al. (2014), Alawode et al. (2011), Moghadam et al. (2012), and Singh et al. (2015). Although the cement content remains unchanged, adding 33% more water significantly alters paste performance, confirming that higher w/c ratios create larger, more connected pores. This increase in porosity directly reduces compressive strength, stiffness, elastic modulus, and durability, as shown in Figure **2.14**.

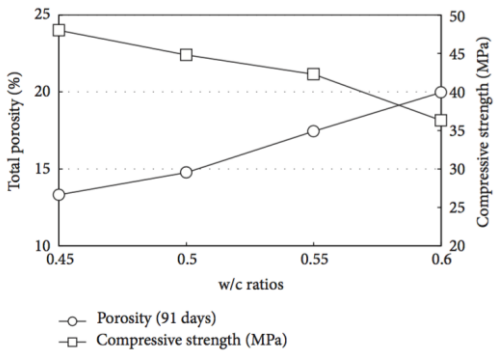

Figure 2.9 Strength and porosity with different w/c ratios (Kim, 2014)

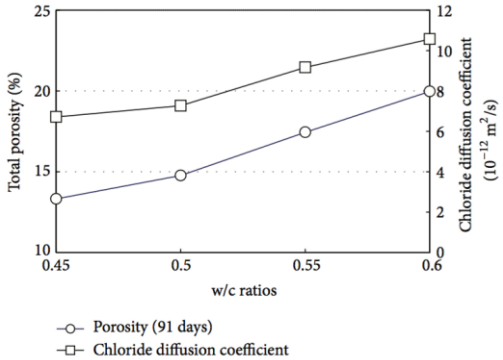

Figure 2.10 Chloride diffusion coefficient and porosity with different w/c ratios (Kim, 2014)

2.5 Recycled Concrete Aggregate (RCA)

Olorunsogo et al. (2002) evaluated the durability of concrete containing recycled aggregate (RA) using indicators such as chloride conductivity, oxygen permeability, and water sorptivity. Three mixtures with 0%, 50%, and 100% RA were tested at 3, 7, 28, and 56 days. The results showed that durability declined as the RA content increased but improved with longer curing, as illustrated in **Figure 2.11**. By 56 days, concrete with 100% RA displayed notably higher durability index values than the natural-aggregate mix—an 86.5% increase in chloride conductivity and a 28.8% increase in water sorptivity..

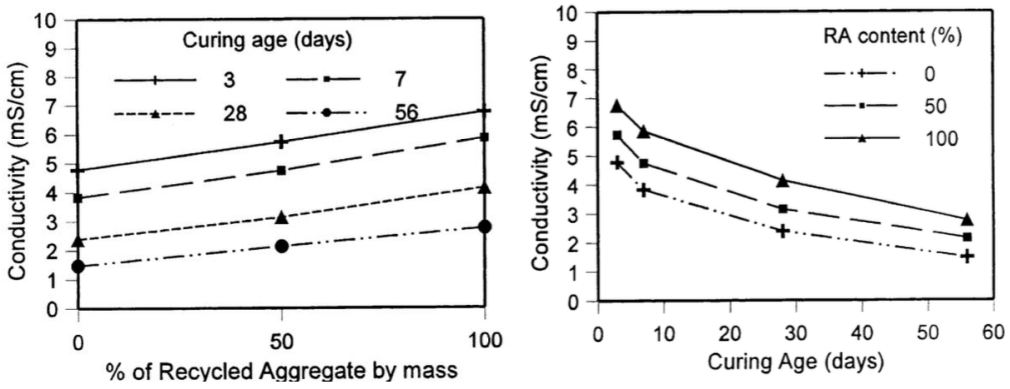

Figure 2.11 Chloride conductivity (Olorunsogo, 2002)

Behera et al. (2014) reported that recycled aggregate (RA) generally shows poor particle size distribution and inadequate grading, largely due to variations introduced by different crushing processes. RA typically contains a higher proportion of fine particles and retains an aged interfacial transition zone (ITZ) from the adhered mortar or cement paste. This ITZ is structurally weak, containing micro-pores, cracks, and fissures formed during crushing, as illustrated in **Figure 2.12**. RA also tends to have a rough, irregular surface and a partially rounded shape due to the attached mortar. Compared with natural aggregate, RA exhibits inferior mechanical properties, including lower crushing strength, reduced impact resistance, and poorer abrasion resistance.

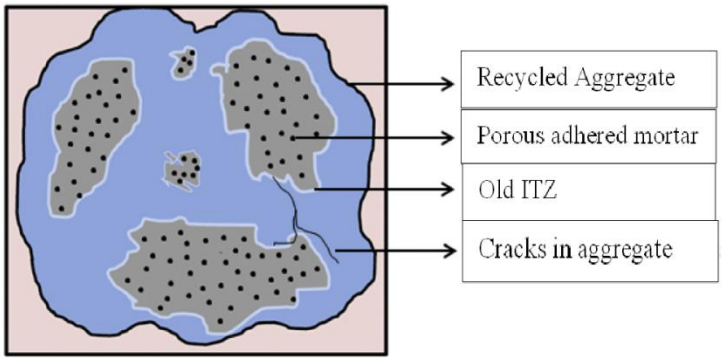

Figure 2.12 Pictorial representation of physical characteristics of recycled aggregate (Bahera, 2014)

Recycled aggregate concrete (RAC) consists of three key phases: the aggregate phase, the mortar phase, and the interfacial transition zones (ITZ)—both between the new matrix and the coarse aggregate and within the adhered mortar. **Figure 2.13a** and b schematically compare these phases in natural aggregate concrete and RAC, highlighting their fundamental differences. Because these phases strongly influence RAC behavior, its performance must be carefully considered when recycled aggregate is incorporated into concrete mixtures.

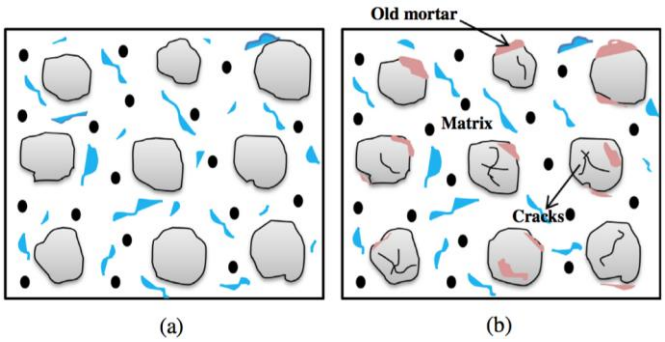

Figure 2.13 Difference between matrixes of (a) natural aggregate concrete and (b) recycle aggregate concrete (Bahera, 2014)

Thomas et al. (2013) investigated the microstructure of recycled aggregate concrete (RAC) using SEM. As shown in **Figure 2.14**, the new cement paste was found

to coat the recycled aggregates, which contain remnants of old paste and natural aggregate. The newly formed paste exhibited a denser and more tightly bonded structure than the original adhered mortar.

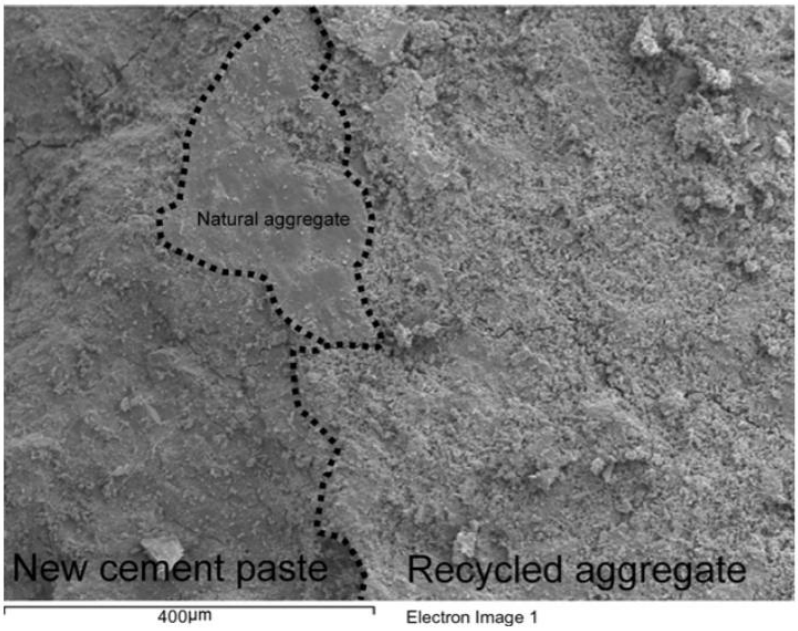

Figure 2.14 Micrograph of RAC structure (Thomas, 2013)

Lee et al. (2013) reported that recycled aggregate concrete (RAC) contains a larger extent of interfacial transition zones (ITZ) than conventional concrete. This is illustrated in **Figure 2.15**, which shows a sectional view emphasizing the ITZ characteristics in RAC.

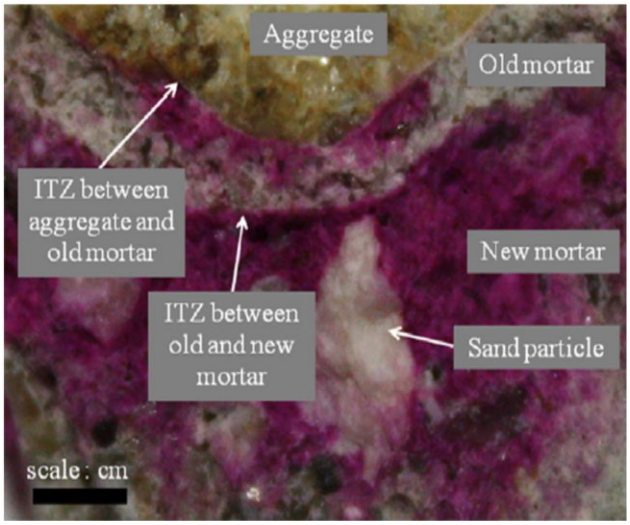

Figure 2.15 Classification of aggregate, old mortar and new mortar by discoloration of phenolphthalein solution (Lee, 2013)

Topcu and Sengel (2008) tested concrete with varying levels of recycled concrete aggregate (RCA), up to 100% replacement. They found that concrete density decreased as RCA content increased, though the change was less pronounced than the corresponding rise in water absorption. **Figure 2.16** summarizes findings from multiple studies, showing a consistent reduction in 28-day compressive strength with higher RA replacement levels.

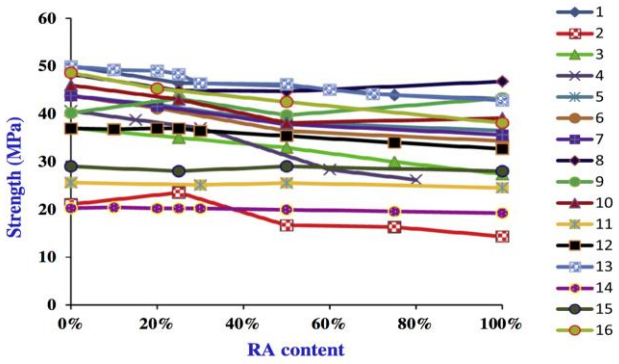

Figure 2.16 Variation in 28 days strength compressive strength w.r.t. RA replacement percentage by various researchers

Tam et al. (2004) introduced the two-stage mixing approach (TSMA) to improve the compressive strength and reduce the variability of recycled aggregate concrete (RAC). Experimental results showed significant strength gains using TSMA. The improvement is attributed to the porous nature of recycled aggregates, where the premixing step helps fill internal pores and cracks, producing a denser matrix and a better interfacial zone than conventional mixing. **Figure 2.17** illustrates the TSMA procedure, while SEM images in **Figures 2.18a and 2.18b** show that cracks within recycled aggregates are effectively filled under TSMA but remain unfilled with normal mixing.

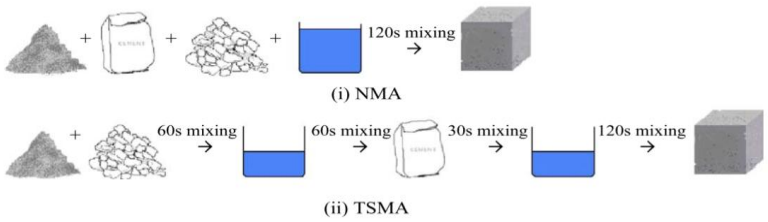

Figure 2.17 Mixing procedures of the (i) normal mixing approach and (ii) two-stage mixing approach (Tam, 2004)

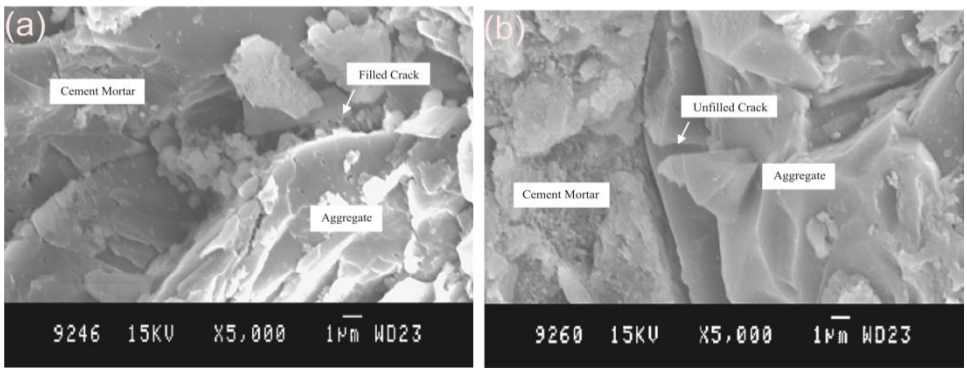

Figure 2.18 (a) Filled crack in RA using TSMA. (b) Unfilled crack in RA using NMA.

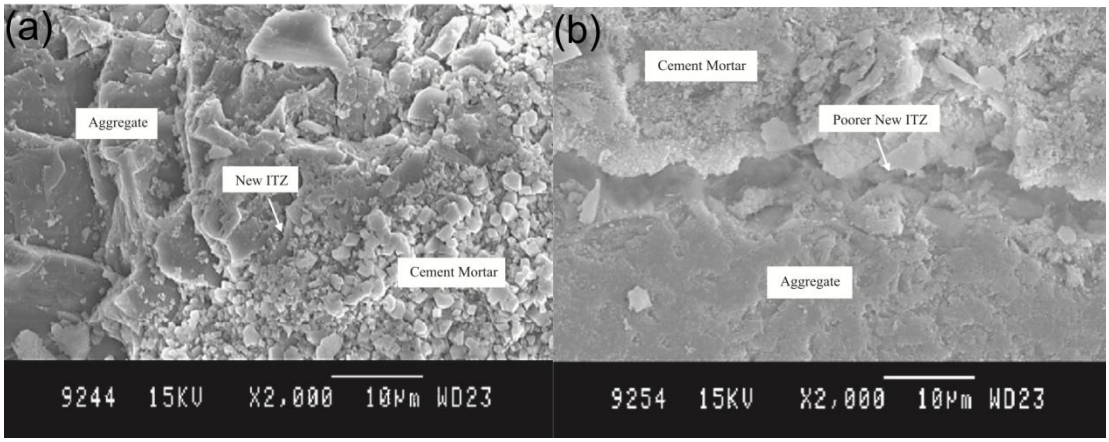

Figure 2.19 (a) New interfacial zone for TSMA. (b) Poorer new interfacial zone for NMA.

Recycled aggregate concrete (RAC) contains both old and new interfacial zones. When the two-stage mixing approach (TSMA) is used, a dense and well-formed new ITZ is observed, as shown in **Figure 2.19a.** In contrast, **Figure 2.19b** shows that normal mixing with natural aggregate (NMA) produces a comparatively weaker ITZ.

Somna et al. (2012) studied the effects of ground fly ash (GFA) and ground bagasse ash (GBA) on the durability of recycled aggregate concrete. In their work, crushed limestone was fully replaced with recycled aggregate, while GFA and GBA were used to substitute Portland cement Type I at 20%, 35%, and 50% of the binder weight. The results showed that both GFA and GBA significantly improved durability. The best performance—in terms of compressive strength, reduced water permeability, and high resistance to chloride penetration and sulfate attack—was achieved at a 20% replacement level. **Figure 2.20** presents the compressive strength of mixes containing GFA (F20, 35, 50) and GBA (B20, 35, 50), and **Figure 2.21** shows the corresponding chloride penetration depths.

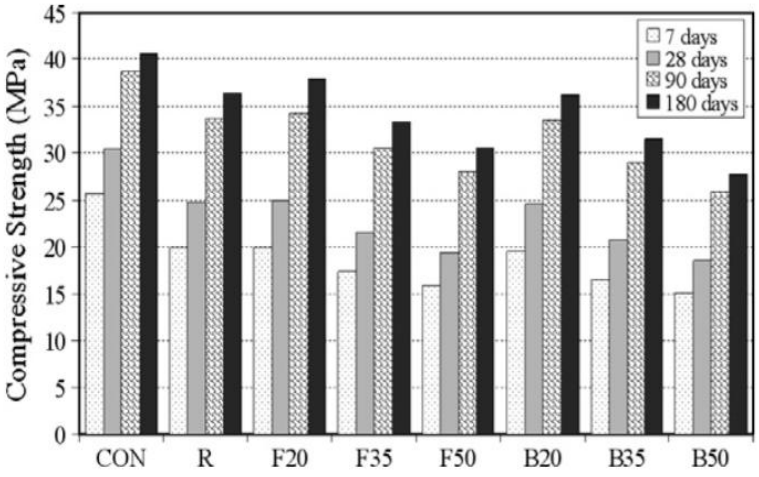

Figure 2.20 Compressive strength of concrete replacement by GFA and GBA

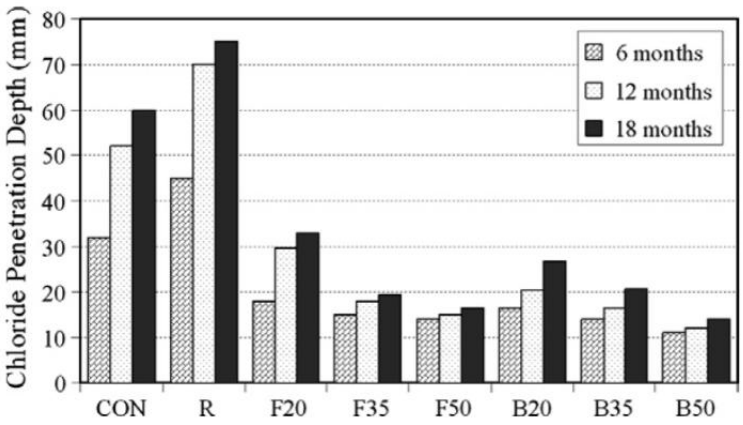

Figure 2.21 Chloride penetration depth of concrete immersed in 3% sodium chloride solution at 6, 12, and 18 months.

Tam et al. (2008) highlighted the improved performance of recycled aggregate (RA) concrete when using the Two-Stage Mixing Approach (TSMA) and a modified version incorporating silica fume and proportional cement content (TSMAsc). In both methods, the premixing step helps fill weak areas within the RA, producing a stronger interfacial layer around the aggregate and increasing concrete strength. The study demonstrates that TSMA and TSMAsc are effective alternatives for enhancing the quality of recycled aggregate, as shown in **Figure 2.22**.

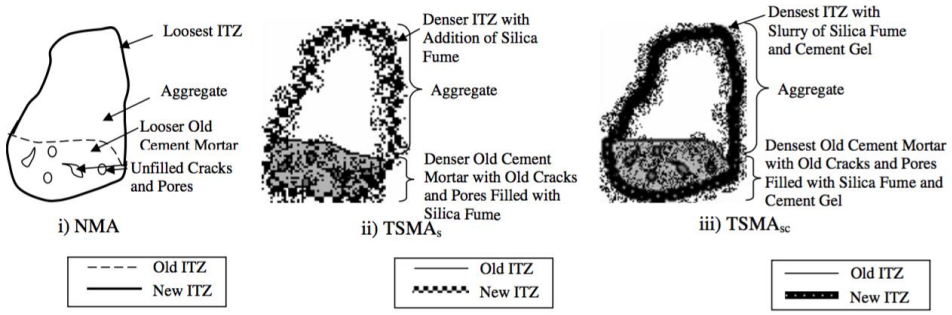

Figure 2.22 RA structure after adopting (i) NMA, (ii) $TSMA_s$ and (iii) $TSMA_{SC}$.

2.6 Natural Rubber Latex (NRL) modified concrete.

Yaowarat et al. (2021) evaluated natural rubber latex (NRL) as a sustainable additive to improve the flexural performance of concrete pavements. The study examined the compressive and flexural strengths of NRL-modified concrete across different water-to-cement (w/c) ratios, dry rubber-to-cement (r/c) ratios, and curing periods. Results showed that compressive strength decreased as the r/c ratio increased for all w/c ratios and curing ages (**Figure 2.23**). In contrast, optimal r/c ratios of 0.58%, 1.16%, and 1.73% for w/c values of 0.3, 0.4, and 0.5, respectively, produced the highest flexural strengths (**Figure 2.24**). Concrete mixtures with w/c ≤ 0.4 and r/c ≤ 2.31, as well as those with w/c = 0.5 and r/c between 0.58 and 1.73, met the compressive and flexural strength requirements of the Department of Highways, Thailand, indicating their suitability for pavement applications.

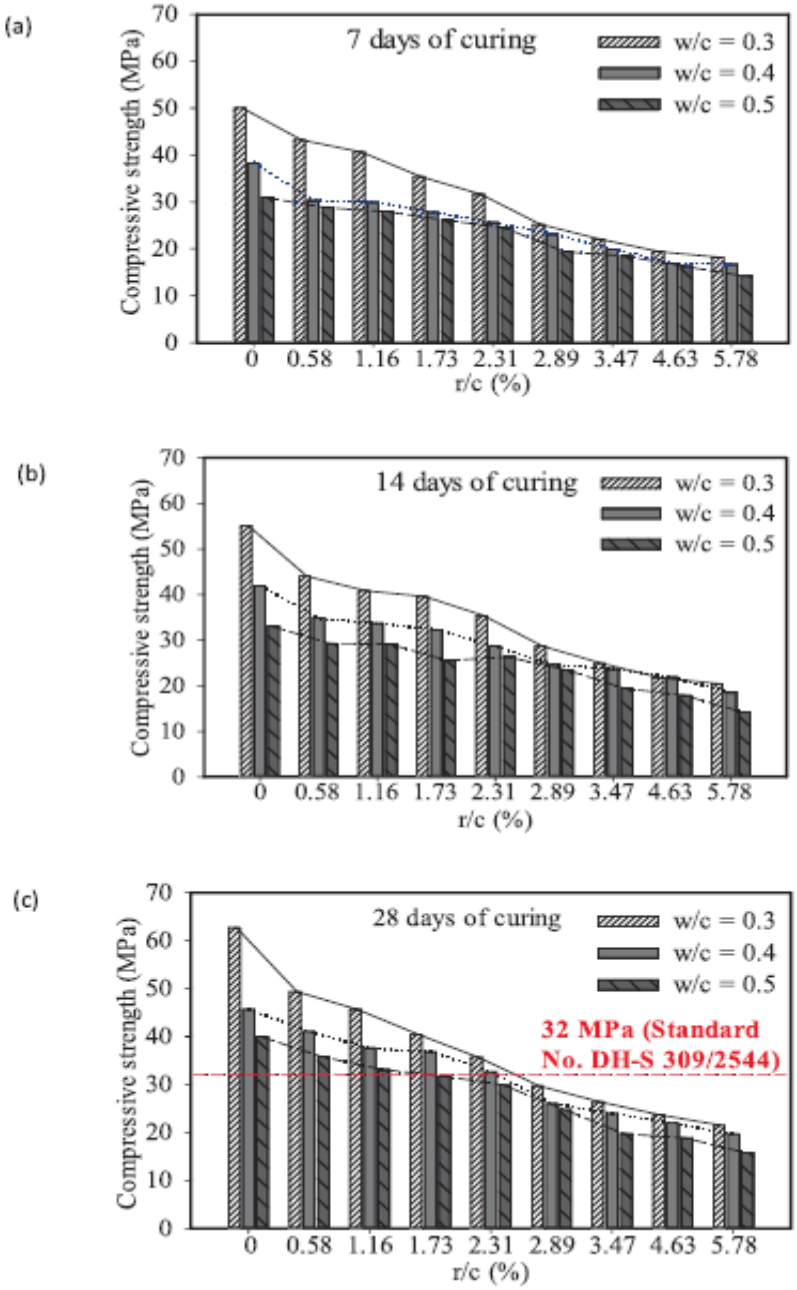

Figure 2.23 Compressive strength of NRL-concrete at (a) 7 days; (b) 14 days; (c) 28 days (Yaowarat et al., 2021)

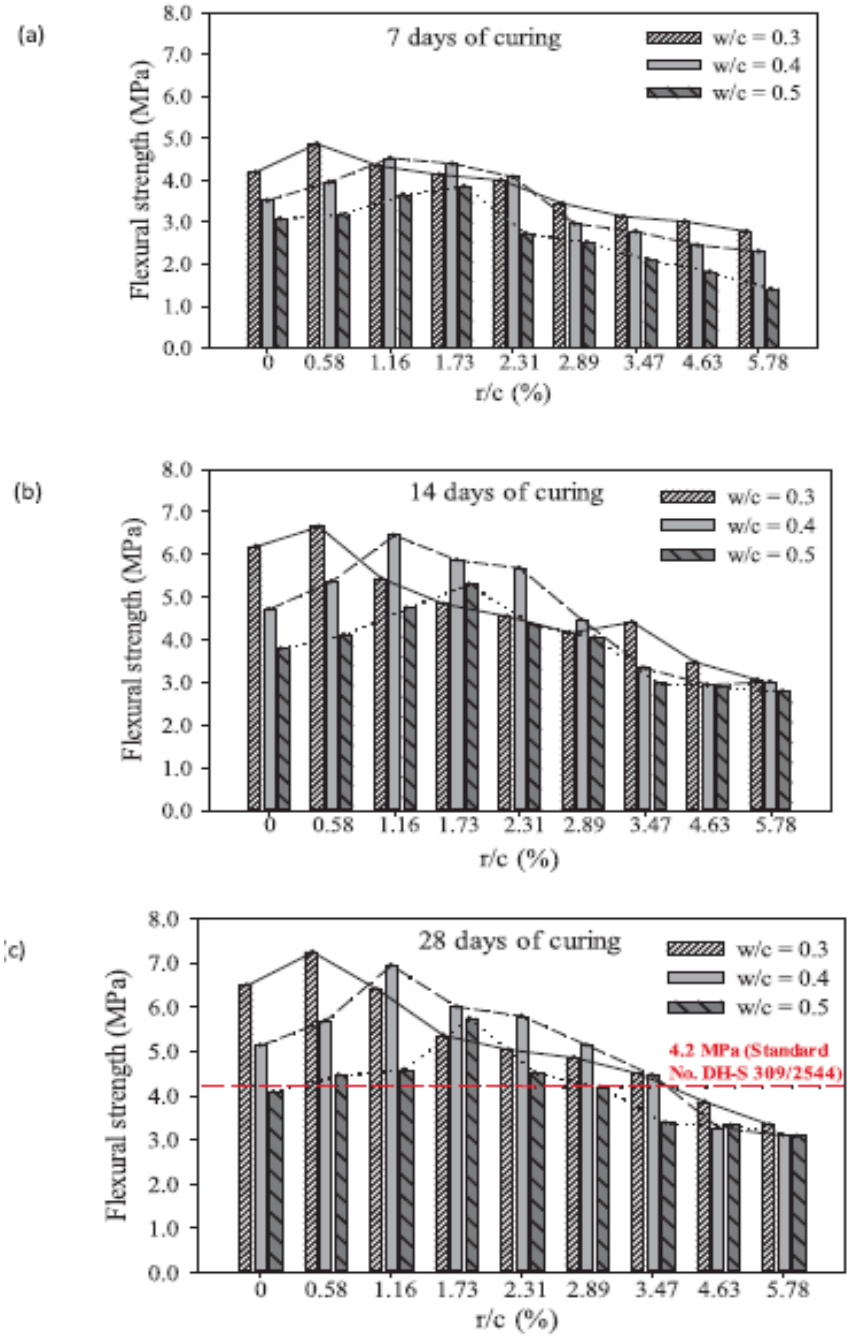

Figure 2.24 Flexural strength of NRL-concrete at (a) 7 days; (b) 14 days; (c) 28 days (Yaowarat et al., 2021)

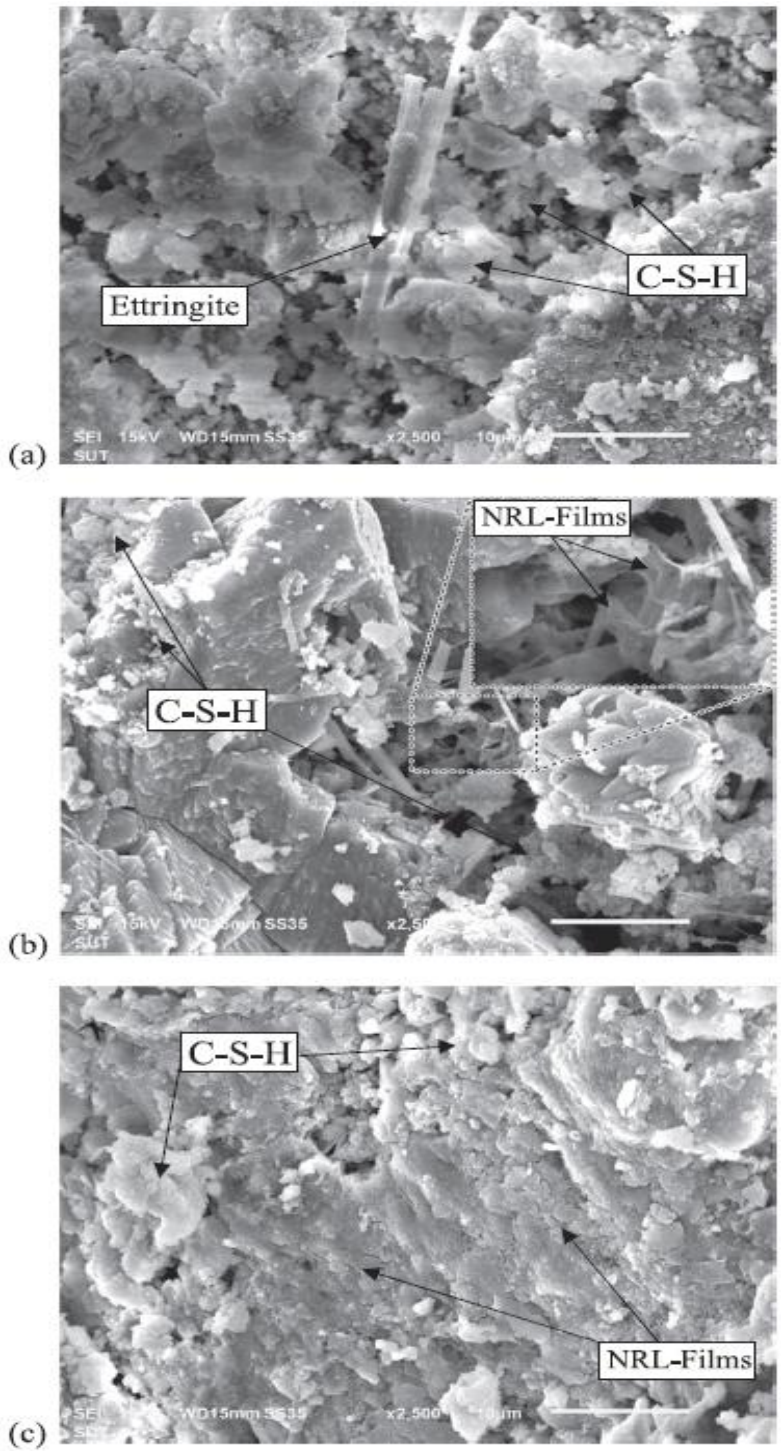

Figure 2.25 SEM images of NRL-concrete for w/c = 0.4 at (a) r/c = 0; (b) r/c = 1.16 (optimal); (c) r/c = 5.78. (Yaowarat et al., 2021)

SEM images showed clear C–S–H gel formation in the normal concrete mix without NRL (**Figure 2.25a**). In NRL-modified specimens, NRL films infiltrated the pore structure (**Figure 2.25b**). At the optimal r/c ratio of 1.16%, thin films were visible within the matrix, while at a higher r/c ratio of 5.78%, thicker films surrounded the C–S–H products (**Figure 2.25c**). These thicker films impeded hydration and reduced the amount of cementitious products, leading to lower compressive strength. Similar behavior has been noted in SEM studies of synthetic polymer–modified concrete.

EDX analysis confirmed the presence of C–S–H and C–A–S–H through the detection of Ca, Si, and Al in all samples (**Figure 2.26**). The highest peak intensities occurred in the control mix (r/c = 0%). As the r/c ratio increased, the intensities of Ca, Si, and Al decreased, with the r/c = 5.78% mix showing the lowest levels. Conversely, carbon content increased with higher NRL content, reflecting the presence of latex. These findings demonstrate that increasing r/c alters the chemical composition and reduces cementitious product formation in NRL-concrete.

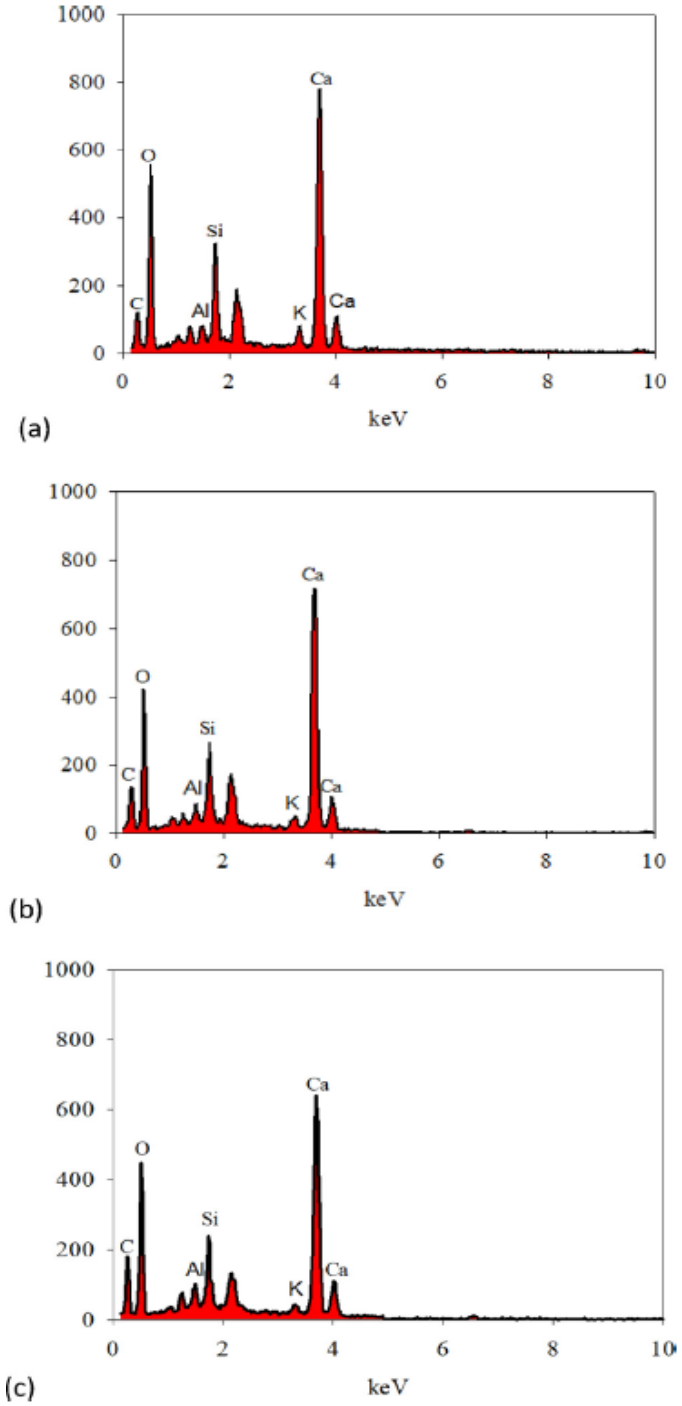

Figure 2.26 EDX results of NRL-concrete for w/c = 0.4 at (a) r/c = 0; (b) r/c = 1.16 (optimal); (c) r/c = 5.78.

Suddeepong et al. (2022) conducted a study to investigate the use of natural rubber latex (NRL) as a means to enhance the mechanical strength and flexural

fatigue resistance of conventional concrete. The study examined the influence of various factors, including the water-to-cement (w/c) ratio and dry rubber-to-cement (r/c) ratio, on the compressive strength, flexural strength, and flexural fatigue behavior of the modified concrete. The results of the study indicate that an increase in the dry rubber-to-cement (r/c) ratio leads to a larger area under the flexural stress-deformation curve, indicating an improvement in flexural toughness. **Figure 2.27** depicts the flexural toughness of NRL-concrete at different water-to-cement (w/c) ratios of 0.3, 0.4, and 0.5, with varying r/c ratios. It is observed that, at the same w/c ratio, the flexural toughness increases with an increasing r/c ratio, reaching its highest value at the optimal r/c ratio for each w/c ratio. However, beyond the optimal r/c ratio, the flexural toughness decreases as the r/c ratio continues to increase..

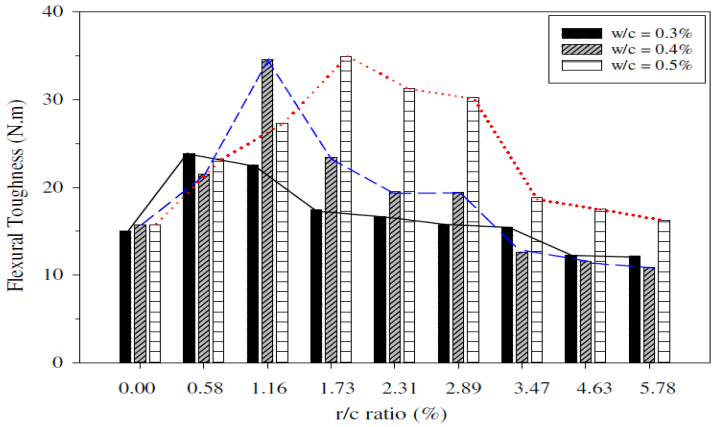

Figure 2.27 Flexural toughness of NRL concrete at different w/c and r/c ratios (Suddeepong et al., 2022)

NRL-concretes with r/c ratios at or below the optimum showed higher fatigue life (Nf) than normal concrete at the same w/c ratio. They also resisted total and plastic deformation more effectively under equivalent stress levels (**Figure 2.28**), exhibiting roughly 45% less plastic deformation than normal concrete.

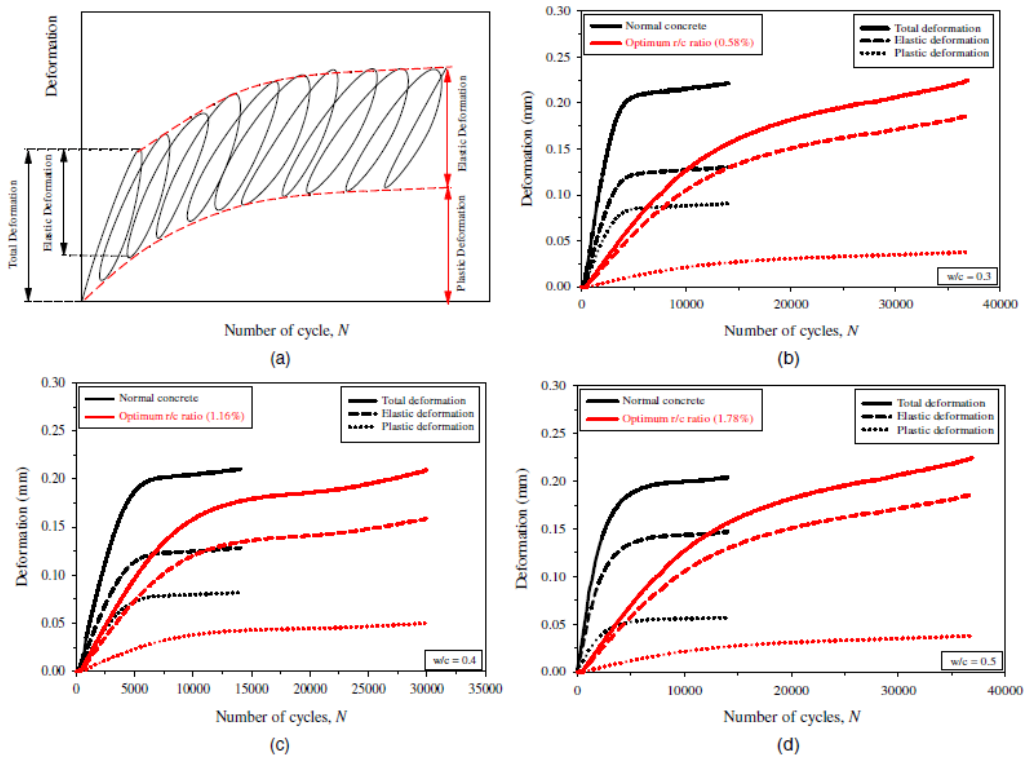

Figure 2.28 Comparation of total, elastic and plastic deformations behavior under repetitive flexural stress of NRL concrete for different r/c ratios at w/c ratio of (a) schematic plot; (b) 0.3%; (c) 0.4%; and (d) 0.5% (Suddeepong et al., 2022)

The study also proposed a stress ratio hypothesis for NRL-concretes, stating that fatigue life remains unchanged as long as the stress ratio (SR) is the same, regardless of differences in w/c ratio, r/c ratio, or pavement thickness. This implies that, for a given target service life, rigid pavements using NRL-modified concrete with r/c values below the optimum can be designed with reduced thickness compared to pavements made with normal concrete (**Figure 2.29**).

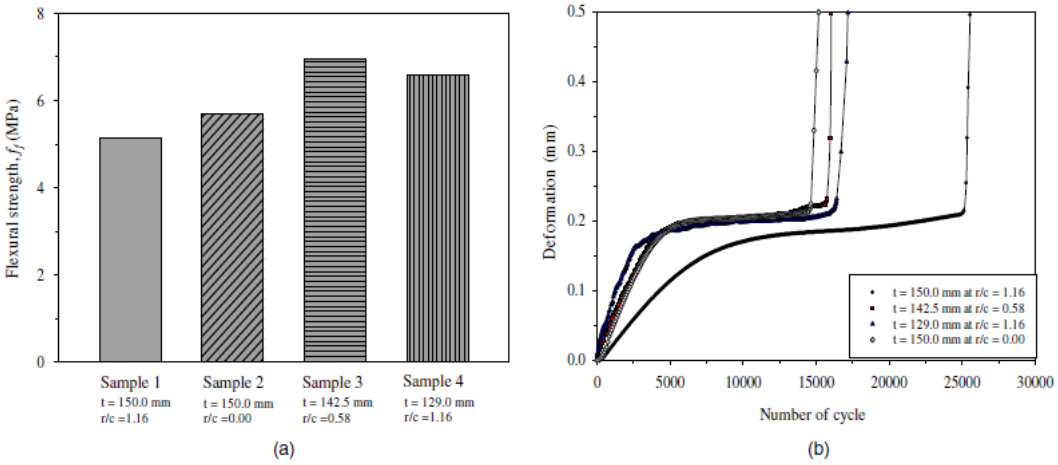

Figure 2.29 (a) Influences of flexural strength on reduction in thickness of normal and NRL concretes; and (b) relationship between deformation and number of cycles at same stress ratio for different thickness and r/c ratios (Suddeepong et al., 2022)

Figure 2.30 shows the relationship between stress ratio (SR) and fatigue life (Nf) for NRL-concretes at different w/c and r/c ratios, compared with the PCA (1984) fatigue model. The NRL-concrete data scatter around the model curve, indicating that SR is a key factor governing fatigue life. The results also show that the PCA fatigue equation can be applied to both normal and NRL-modified concrete pavements.

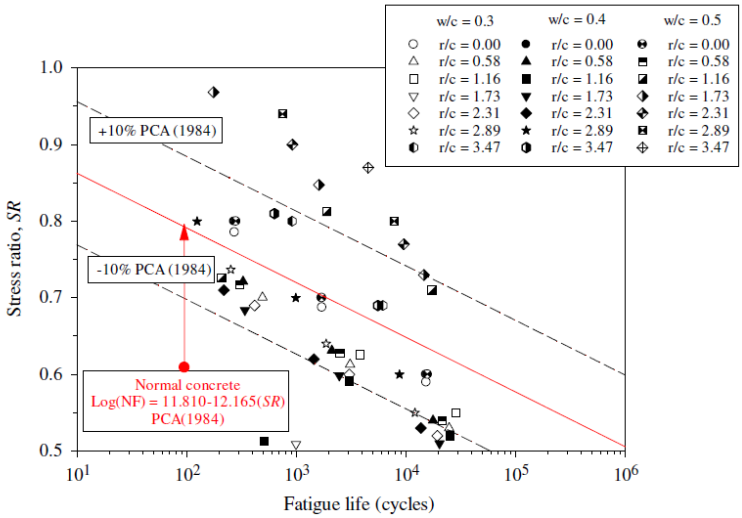

Figure 2.30 Relationship between stress ratio and fatigue life of normal and NRL-concretes at different w/c and r/c ratios (Suddeepong et al., 2022)

Muhammad and Ismail (2012) examined the microstructure of several concrete mixes—normal mix (NM), modified mixes (MM-10% and MM-20%), and latex film. The NM showed noticeable voids and gaps at the interface between cement oxides and aggregate particles, reflecting the typical porosity of conventional concrete (**Figure 2.31a**). In contrast, the modified mixes were more compact, with compaction increasing as latex content increased. MM-10% displayed a denser texture than NM (**Figure 2.31b**), while MM-20% effectively filled voids and coated the surfaces of cement oxides and aggregates, producing a structure with minimal inter-particle gaps (**Figure 2.31c**).

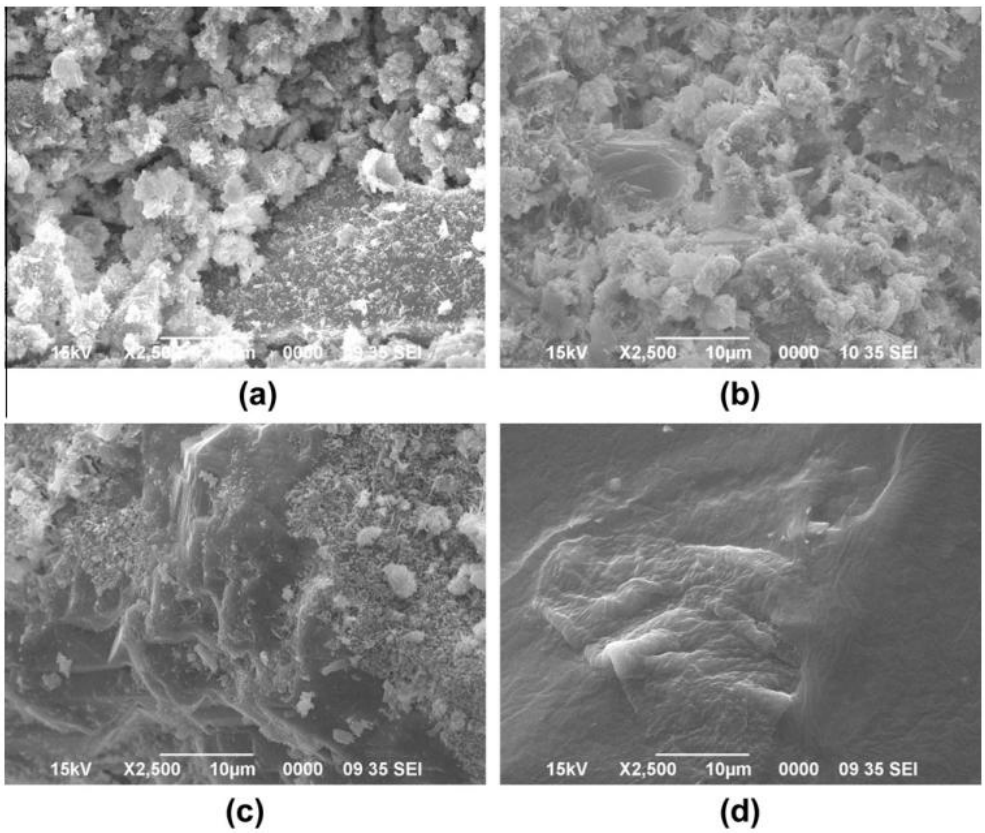

Figure 2.31 Morphologies; (a) normal cement-sand matrix, (b) cement-sand with 10% latex, (c) cement-sand with 20% latex and (d) latex-film (Muhammad and Ismail, 2012)

The latex film itself exhibited a fine, grain-textured membrane (**Figure 2.31d**). In its liquid form, natural rubber latex (NRL) contains dispersed poly-1,4-isoprene particles, but as the water phase drains, the particles draw closer and eventually coalesce into a continuous film. When NRL is added to concrete in small amounts, however, full film formation is less likely; instead, clusters of isoprene particles may accumulate within capillary pores and voids.

2.7 Fly Ash (FA) modified concrete.

Fly ash (FA) is a finely divided residue generated from the combustion of pulverized coal in thermal power plants and has been widely utilized as a supplementary cementitious material in concrete. Its incorporation into concrete has attracted significant attention due to both its technical benefits and its contribution to sustainable construction. FA typically consists of spherical particles rich in amorphous silica and alumina, which can react with calcium hydroxide produced during cement hydration to form additional calcium silicate hydrate (C–S–H) gel through pozzolanic reactions. This secondary C–S–H formation plays a crucial role in refining pore structure, enhancing microstructural densification, and improving long-term performance of concrete.

From a fresh-state perspective, FA generally improves workability due to its spherical particle shape and ball-bearing effect, which reduces internal friction among solid particles. This characteristic is particularly beneficial in mixtures containing recycled concrete aggregate (RCA), which typically exhibits rough surface texture and high water absorption. The improved workability provided by FA can reduce water demand, thereby helping to control the water-to-binder ratio and mitigate the adverse effects associated with RCA incorporation.

In terms of mechanical properties, FA-modified concrete often exhibits lower early-age strength compared to conventional Portland cement concrete due to the slower kinetics of pozzolanic reactions. However, at later ages, the continued reaction between FA and calcium hydroxide leads to progressive strength gain, which can equal or exceed that of control mixtures. This long-term strength development is particularly advantageous for rigid pavement applications, where durability and

sustained load-carrying capacity are more critical than early-age strength alone. Moreover, the refined microstructure resulting from FA incorporation enhances the interfacial transition zone (ITZ) between aggregates and cement paste, contributing to improved mechanical performance.

Durability enhancement is another major benefit of FA-modified concrete. The reduction in calcium hydroxide content and pore connectivity leads to lower permeability, which improves resistance to chloride ingress, sulfate attack, and alkali–silica reaction. These durability improvements are essential for pavement concrete exposed to aggressive environmental conditions, repeated traffic loading, and moisture fluctuations. In RCA-based concrete, FA further contributes to mitigating the negative effects of residual mortar by densifying the cementitious matrix and improving ITZ quality.

From an environmental standpoint, FA plays a pivotal role in reducing the carbon footprint of concrete. Cement production is the dominant source of CO_2 emissions in concrete, and partial replacement of cement with FA directly lowers embodied carbon. In addition, FA utilization promotes waste valorization by diverting industrial by-products from landfills and reducing the demand for energy-intensive clinker production. When evaluated through life-cycle-oriented indicators, FA-modified concrete consistently demonstrates lower CO_2-equivalent emissions compared to conventional concrete mixtures.

Economic considerations further support the adoption of FA-modified concrete. FA is generally less expensive than Portland cement, and its use can reduce overall material cost while maintaining or enhancing long-term performance. In pavement applications, improved durability and fatigue resistance associated with FA incorporation may also contribute to extended service life and reduced maintenance frequency, resulting in lower life-cycle costs.

Despite these advantages, the performance of FA-modified concrete is highly dependent on replacement level, curing conditions, and interaction with other mix constituents. Excessive FA replacement may lead to insufficient early-age strength, particularly when combined with other materials that retard hydration. Therefore, careful optimization of FA content is essential, especially in multi-component systems

incorporating recycled aggregates and polymer modifiers. When properly designed, FA-modified concrete represents a key component in the development of low-carbon, durable, and cost-effective rigid pavement materials aligned with sustainable infrastructure goals.

2.8 References

Ait-Aider, H., Hannachi, N. E., & Mouret, M. (2007). **Importance of W/C ratio on compressive strength of concrete in hot climate conditions. Building and Environment**, 42(6), 2461-2465.

Ajdukiewicz, A., & Kliszczewicz, A. (2002). **Influence of recycled aggregates on mechanical properties of HS/HPC**. Cement and concrete composites, 24(2), 269-279.

Alawode, O., & Idowu, O. I. (2011). **Effects of water-cement ratios on the compressive strength and workability of concrete and lateritic concrete mixes**. The Pacific Journal of Science and Technology, 12(2), 99-105.

Albano, C., Camacho, N., Hernandez, M., Matheus, A., & Gutierrez, A. (2009). **Influence of content and particle size of waste pet bottles on concrete behavior at different w/c ratios**. Waste Management, 29(10), 2707-2716.

Behera, M., Bhattacharyya, S. K., Minocha, A. K., Deoliya, R., & Maiti, S. (2014). **Recycled aggregate from C&D waste & its use in concrete–A breakthrough towards sustainability in construction sector: A review**. Construction and building materials, 68, 501-516.

Buck, A. D. (1977, May). **Recycled concrete as a source of aggregate.** In Journal Proceedings (Vol. 74, No. 5, pp. 212-219).

Buyle-Bodin, F., & Hadjieva-Zaharieva, R. (2002). **Influence of industrially produced recycled aggregates on flow properties of concrete**. Materials and Structures, 35(8), 504-509.

Ceia, F., Raposo, J., Guerra, M., Júlio, E., & de Brito, J. (2016). **Shear strength of recycled aggregate concrete to natural aggregate concrete interfaces.** Construction and Building Materials, 109, 139-145.

Choi, W. H., Ghorpade, P. A., Kim, K. B., Shin, J. W., & Park, J. Y. (2012). **Properties of synthetic monosulfate as a novel material for arsenic removal.** Journal of hazardous materials, 227, 402-409.

Diamond S., **The Microstructures of cement paste in concrete**, 8th ICCCC. Vol. 1 pp. 113-121, Rio de Janeiro (1986)

Dosho, Y. (2007). **Development of a Sustainable Concrete Waste Recycling System-Application of Recycled Aggregate Concrete Produced by Aggregate Replacing Method**. Journal of Advanced Concrete Technology, 5(1), 27-42.

Elhakam, A. A., Mohamed, A. E., & Awad, E. (2012). **Influence of self-healing, mixing method and adding silica fume on mechanical properties of recycled aggregates concrete.** Construction and Building Materials, 35, 421-427.

Etxeberria, M., Vázquez, E., Marí, A., & Barra, M. (2007). **Influence of amount of recycled coarse aggregates and production process on properties of recycled aggregate concrete**. Cement and concrete research, 37(5), 735-742.

FHWA. (2004). **Transportation application of recycled concrete aggregate.** United States of America: Federal Highway Administration.

Franus, W., Panek, R., & Wdowin, M. (2015). **SEM investigation of microstructures in hydration products of portland cement**. In 2nd International Multidisciplinary Microscopy and Microanalysis Congress (pp. 105-112). Springer International Publishing.

Frías, M., Rodriguez, O., Vigil de la Villa, R., García, R., Martínez-Ramiréz, S., Fernández-Carrasco, L. J. and Vegas, I. (2016), **The Influence of Activated Coal Mining Wastes on the Mineralogy of Blended Cement Pastes**. J. Am. Ceram. Soc., 99: 300–307. doi:10.1111/jace.13840

Goncalves A, Esteves A. Vieira M. **Influence of Recycled Concrete Aggregates on concrete durability. In: RILEM proceedings PRO 40: use of recycled** materials in buildings and structures; 2004.

Grosskurth, K. P., **Materials Research Society Symposium Proceedings: Specialty Cements withAdvanced Properties** 179:273- 281, Materials Research Society, Pittsburgh (1991)

Gutiérrez, A. (2004). **Influence of attached mortar content on the properties of recycled concrete aggregate.** In E. Vázquez, C. F. Hendriks, & G. M. T. Janssen (Eds.), International RILEM Conference on the Use of Recycled Materials in Building and Structures (pp. 536-544). RILEM Publications SARL.

Hansen, T. C., & Boegh, E. (1985, September). **Elasticity and drying shrinkage concrete of recycled-aggregate.** In Journal Proceedings (Vol. 82, No. 5, pp. 648-652).

Hansen, T. C., & Narud, H. (1983). **Strength of recycled concrete made from crushed concrete coarse aggregate**. Concrete International, 5(01), 79-83.

Hassan, CM., and Peppas, NA. (2000). "**Structure and morphology of freeze/thawed PVA hydrogels.**" Macromolecules., 33(7), 2472-2479.

Ismail, S., & Ramli, M. (2013). **Engineering properties of treated recycled concrete aggregate (RCA) for structural applications**. Construction and building Materials, 44, 464-476.

Kim, Y. Y., Lee, K. M., Bang, J. W., & Kwon, S. J. (2014). **Effect of W/C ratio on durability and porosity in cement mortar with constant cement amount.** Advances in Materials Science and Engineering, 2014.

Knapen, E., & Van Gemert, D. (2009). **Cement hydration and microstructure formation in the presence of water-soluble polymers**. Cement and Concrete Research, 39(1), 6-13.

Kou, S. C., & Poon, C. S. (2008). **Mechanical properties of 5-year-old concrete prepared with recycled aggregates obtained from three different sources.** Magazine of Concrete Research, 60(1), 57-64.

Kou, S. C., & Poon, C. S. (2012). **Enhancing the durability properties of concrete prepared with coarse recycled aggregate**. Construction and Building Materials, 35, 69-76.

Kou, S. C., Poon, C. S., & Chan, D. (2004, November). **Properties of steam cured recycled aggregate fly ash concrete.** In International RILEM conference on the use of recycled materials in buildings and structures, Barcelona (pp. 590-599).

Kou, S. C., Poon, C. S., & Chan, D. (2007). **Influence of fly ash as cement replacement on the properties of recycled aggregate concrete**. Journal of Materials in Civil Engineering, 19(9), 709-717.

Kwan, W. H., Ramli, M., Kam, K. J., & Sulieman, M. Z. (2012). **Influence of the amount of recycled coarse aggregate in concrete design and durability properties.** Construction and Building Materials, 26(1), 565-573.

Laserna, S., & Montero, J. (2016). **Influence of natural aggregates typology on recycled concrete strength properties**. Construction and Building Materials, 115, 78-86.

Lee, G. C., & Choi, H. B. (2013). **Study on interfacial transition zone properties of recycled aggregate by micro-hardness test**. Construction and Building Materials, 40, 455-460.

Lerch, W. (2008). **The influence of gypsum on the hydration and properties of Portland cement pastes** (No. SP-249-6).

Suddeepong, A., Buritatum, A., Hoy, M., Horpibulsuk, S., Takaikaew, T., Horpibulsuk, J., & Arulrajah, A. (2022). **Natural Rubber Latex–Modified Concrete Pavements: Evaluation and Design Approach.** Journal of Materials in Civil Engineering, 34(9), 04022215.

Sun, H., Li, Z., Memon, S. A., Zhang, Q., Wang, Y., Liu, B., ... & Xing, F. (2015). **Influence of ultrafine 2CaO· SiO2 powder on hydration properties of reactive powder concrete.** *Materials*, *8*(9), 6195-6207.

Limbachiya, M. C., Koulouris, A., Roberts, J. J., & Fried, A. N. (2004). **Performance of recycled aggregate concrete.** In Proceeding of RILEM International Symposium on Environment-Conscious Materials and Systems for Sustainable Development (pp. 127-136).

Limbachiya, M. C., Leelawat, T., & Dhir, R. K. (2000). **Use of recycled concrete aggregate in high-strength concrete.** Materials and structures, 33(9), 574.

Limbachiya, M., Meddah, M. S., & Ouchagour, Y. (2012). **Performance of Portland/Silica Fume Cement Concrete Produced with Recycled Concrete Aggregate.** ACI Materials Journal, 109(1).

Locher R., Richartz W., **Study of hydration mechanism of cement**. Symp. Chem. Cement

Ma, H., Xu, B., Liu, J., Pei, H., & Li, Z. (2014). **Effects of water content, magnesia-to-phosphate molar ratio and age on pore structure, strength and permeability of magnesium potassium phosphate cement paste**. Materials & Design, 64, 497-502.

Mehta, P. K. (1986). **Concrete. Structure, properties and materials**.

Moghadam, H. A., & Khoshbin, O. A. (2012). **Effect of Water-Cement Ratio (w/c) on Mechanical Properties of Self-Compacting Concrete (Case Study).** World Academy of Science, Engineering and Technology, International Journal of Civil, Environmental, Structural, Construction and Architectural Engineering, 6(5), 317-320.Moscow, Moscow, Russia (1974)

Muhammad, B., & Ismail, M. (2012). **Performance of natural rubber latex modified concrete in acidic and sulfated environments**. Construction and Building Materials, 31, 129-134.

Ohama, Y. (1995). **Handbook of polymer-modified concrete and mortars: properties and process technology**. William Andrew.

Olorunsogo, F. T., & Padayachee, N. (2002). **Performance of recycled aggregate concrete monitored by durability indexes**. Cement and Concrete Research, 32(2), 179-185.

Otsuki, N., Miyazato, S. I., & Yodsudjai, W. (2003). **Influence of recycled aggregate on interfacial transition zone, strength, chloride penetration and carbonation of concrete.** Journal of materials in civil engineering, 15(5), 443-451.

Park C, Sim J. **Fundamental properties of concrete using recycled concrete aggregate produced through advanced recycling process**. Transportation research board 85th annual meeting, Washington, DC, USA; 22–26 January 2006

Poon, C. S., Shui, Z. H., & Lam, L. (2004). **Effect of microstructure of ITZ on compressive strength of concrete prepared with recycled aggregates.** Construction and Building Materials, 18(6), 461-468.

Poon, C. S., Shui, Z. H., Lam, L., Fok, H., & Kou, S. C. (2004). **Influence of moisture states of natural and recycled aggregates on the slump and compressive strength of concrete.** Cement and concrete research, 34(1), 31-36.

Rao, A., Jha, K. N., & Misra, S. (2007). **Use of aggregates from recycled construction and demolition waste in concrete. Resources, conservation and Recycling**, 50(1), 71-81.

Rao, M. C., Bhattacharyya, S. K., & Barai, S. V. (2011). **Influence of field recycled coarse aggregate on properties of concrete. Materials and Structures**, 44(1), 205-220.

Shi, C., Li, Y., Zhang, J., Li, W., Chong, L., & Xie, Z. (2015). **Performance enhancement of recycled concrete aggregate e A review**. Journal of Cleaner Production, 30, 1e7.

Singh, S. B., Munjal, P., & Thammishetti, N. (2015). **Role of water/cement ratio on strength development of cement mortar.** Journal of Building Engineering, 4, 94-100.

Somna, R., Jaturapitakkul, C., & Amde, A. M. (2012). **Effect of ground fly ash and ground bagasse ash on the durability of recycled aggregate concrete**. Cement and Concrete Composites, 34(7), 848-854.

Sri Ravindrajah, R., Loo, Y. H., & Tam, C. T. (1988). **Strength evaluation of recycled-aggregate concrete by in-situ tests.** Materials and Structures, 21(4), 289-295.

Sri, R., & Tam, C. T. (1985). **Properties of concrete made with crushed concrete as coarse aggregate.** Magazine of Concrete Research, 37(130).

Sugita, J., Takagi, S., Mashino, M., and Sakai, E., **Extended Abstracts: The 47th Annual Meeting of JCA**, pp. 74-79, Japan Cement Association, Tokyo (Apr. 1993.

Sun, Hongfang; Li, Zishanshan; Bai, Jing; Memon, Shazim A.; Dong, Biqin; Fang, Yuan; Xu, Weiting; Xing, Feng. 2015. "**Properties of Chemically Combusted Calcium Carbide Residue and Its Influence on Cement Properties**." Materials 8, no. 2: 638-651.

Tam, V. W., & Tam, C. M. (2008). **Diversifying two-stage mixing approach (TSMA) for recycled aggregate concrete: TSMAs and TSMAsc.** Construction and Building Materials, 22(10), 2068-2077.

Tam, V. W., Gao, X. F., & Tam, C. M. (2005). **Microstructural analysis of recycled aggregate concrete produced from two-stage mixing approach**. Cement and concrete research, 35(6), 1195-1203.

Tangchirapat, W., Khamklai, S., & Jaturapitakkul, C. (2012). **Use of ground palm oil fuel ash to improve strength, sulfate resistance, and water permeability of concrete containing high amount of Recycled Concrete Aggregates**. Materials & Design, 41, 150-157.

Yaowarat, T., Suddeepong, A., Hoy, M., Horpibulsuk, S., Takaikaew, T., Vichitcholchai, N., Arulrajah, A. & Chinkulkijniwat, A. (2021). **Improvement of flexural strength of concrete pavements using natural rubber latex**. Construction and Building Materials, 282, 122704.

Thomas, C., Setién, J., Polanco, J., Alaejos, P., & De Juan, M. S. (2013). **Durability of recycled aggregate concrete.** Construction and Building Materials, 40, 1054-1065.

Wang, S., Baxter, L., & Fonseca, F. (2008). **Biomass fly ash in concrete: SEM, EDX and ESEM analysis.** Fuel, 87(3), 372-379.